The 2010 IEEE/RSJ International Conference on
Intelligent Robots and Systems
October 18-22, 2010, Taipei, Taiwan

A Mobile Robot that Understands Pedestrian Spatial Behaviors

Shu-Yun Chung and Han-Pang Huang, *Member, IEEE*

***Abstract*— In human society, there are many invisible social rules or spatial effects existing in our environments. The robot that does not comprehend these spatial effects might harm people or itself. This paper presents a spatial behavior cognition model (SBCM) to describe the spatial effects existing between people and people, people and environments. By understanding the spatial effects in human-lived environments, the robot not only predicts pedestrian intentions and trajectories but also behaves socially acceptable motions. Moreover, the concept of pedestrian ego-graph (PEG) is proposed to efficiently query pedestrian-like paths for trajectory prediction. Model evaluation and experiments are shown to verify the proposed idea in this paper.**

I. Introduction

TODAY robots are no longer only operated in laboratories or factories. Lots of novel robots were designed to work in the populated or outdoor environments. In the near future, more and more robots will appear in our human society. To make robots "smoothly" coexist and share the environments with humans, robots should try to understand human behaviors and execute socially acceptable motions.

In this paper, behavior understanding mainly targets at spatial interactions. A factor which can affect the pedestrian behaviors is represented as a spatial effect in this paper. There are many social rules or implicit "spatial effects" existing in human society. Pedestrians usually have high-level cognition to reason, infer, and interact with the environments in "appropriate" ways (Fig. 1). In other words, the environments seem to generate some "spatial effects" that force pedestrians to perform certain motions. Our purpose is to make robots understand these spatial effects and further predict pedestrian intentions or behave human-like motions. However, these spatial effects are usually invisible and immeasurable by sensors. It leads spatial effect understanding into a difficult task. Fortunately, people sometimes interpret their feelings or intentions through non-verbal communications such as their paths, postures, facial expressions, and eye contact etc. We are able to infer the spatial effects by observing pedestrian behaviors. Previous researches also studied the spatial interactions between people and robots [8, 10, 12].

This work is partially supported by the Industrial Development Bureau, Ministry of Economic Affairs of R.O.C. under grants 97-222-1-E-002-161-MY3 97C1031-2.

Shu Yun Chung is currently a Ph.D. student in Department of Mechanical Engineering, National Taiwan University, Taipei, Taiwan (e-mail: f91522803@ntu.edu.tw).

Han Pang Huang is a professor of Department of Mechanical Engineering, National Taiwan University, Taipei, Taiwan (phone: 886-2-33664478; fax: 886-2-23676064; e-mail: hanpang@ntu.edu.tw).

(a) (b)

Fig. 1 Some social rules and spatial effects existing in human society, (a) pedestrians usually stand to one side of the escalator to allow others to rapidly pass, (b) people naturally keep the social distance between groups.

However, most of these works were limited to certain situations or behaviors. They lacked a generalized framework for describing the relationships between different spatial effects.

This paper mainly contributes two points. At first, the concept of pedestrian ego-graph (PEG) is represented. PEG is created based on the statistical results from collected trajectories of pedestrians and is utilized to rapidly generate pedestrian-like path for trajectory prediction. Second, the framework of spatial behavior cognition model (SBCM) is proposed to describe the spatial effects in most human-lived environments. The robot is further able to comprehend and incrementally detect new spatial effects through SBCM.

This paper is organized as follows. In section II, the structure of PEG is introduced. SBCM and spatial effects learning are discussed from section III to V. In section VI, the probability model of prediction is derived. The model evaluation and the experiment are demonstrated in section VII. The conclusions are summarized in section VIII.

II. Pedestrian Ego-Graph

In general, it is not easy to rapidly predict the pedestrian trajectory in highly dynamic environments. Most developed methods [6, 13] only consider the reactive social forces which generate the next action of the pedestrian based on current observations. It is usually suited for the tracking problem but not the prediction problem. Because of its greedy property, this kind of methods may fail in long term prediction and get blocked in the areas with local minimum cost. Although some algorithms were proposed for long term prediction [2-3, 14], they ignored the spatial effect between pedestrians and cannot model the avoidance behaviors between pedestrians. This paper presents the concept of pedestrian ego-graph (PEG) to overcome this drawback.

An ego-graph [9] is a local motion planning approach used in the field of mobile robots, especially for the robots with motion constraints [7]. It is a graph that gathers several possible robot states and generates different trajectories

through these states by considering kinematics and dynamics constraints. Since each trajectory is only associated to certain states, it is able to efficiently score all the trajectories on-line and choose one of trajectories for the next motion strategy.

In daily life, pedestrians usually adopt similar strategies to avoid obstacles. Thus we utilize the concept of ego-graph to predict pedestrian trajectories. On the other hand, ego-graph also retains the characteristic of multiple hypotheses which is helpful to create the probability model of prediction. The procedure for building the PEG from collected trajectories is discussed below.

At first, 770 trajectories are collected from 6 different places including indoor and outdoor environments. The moving direction of the initial state in each trajectory is rotated to the upward direction (Fig. 2(a)). Each trajectory is divided into several trajectory pieces with lengths of 7~9 m. In this case, 2669 trajectory pieces are obtained.

63 partitions distributed in 3 layers are defined depending on the radial distance and orientation to the center of PEG (Fig. 2(b)). 3 partitions from different layers become one partition set. Thus 1259 partition sets are generated in the preliminary PEG. According to the location in the PEG, each trajectory piece fits into one of the partition sets. From the statistical results, partition sets with fewer trajectory pieces are removed. Finally, only 49 partitions and 243 partition sets are reserved. Moreover, the statistical trajectory clustering method [4] is utilized to estimate the regression model of trajectories in each partition set (Fig. 3).

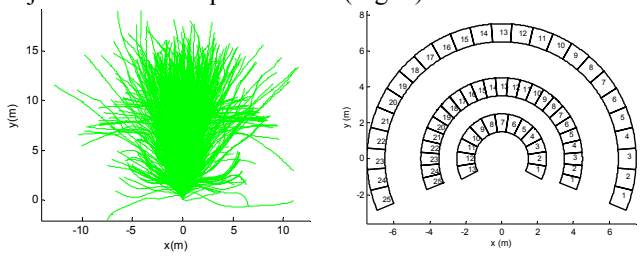

(a) (b)

Fig. 2 (a) 770 trajectories are collected, (b) preliminary partition distribution

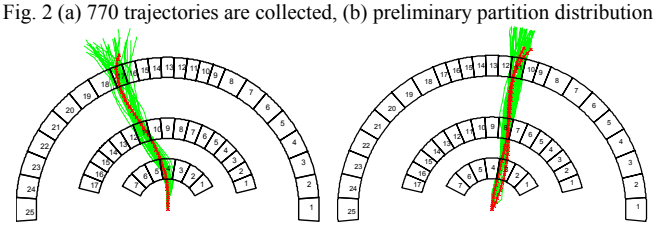

(a) (b)

Fig. 3 Trajectory clustering and regression (a) the red curve shows the regressive trajectory in one partition set, (b) sometimes two regressive trajectories appear in one partition set.

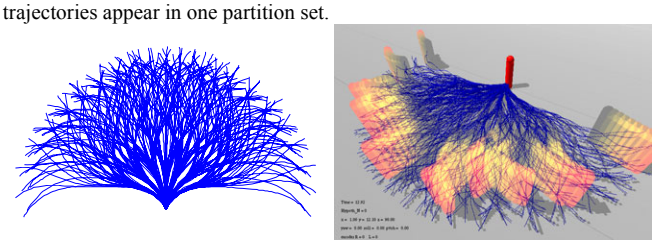

(a) (b)

Fig. 4 (a) pedestrian ego graph (PEG), (b) PEG can rapidly generate multiple hypotheses for trajectory prediction.

The regressive trajectories in each partition are regarded as the policies of pedestrians. At the final, 248 trajectories are shown in pedestrian ego-graph as shown in Fig. 4.

III. Spatial Behavior Cognition Model (SBCM)

We assume the pedestrian spatial behaviors are influenced by some spatial effects existing in the environments. According to the frequency of occurrence, the spatial effects are classified into general spatial effects (GSEs) and specific spatial effects (SSEs). GSEs usually exist in most environments and represent the basic spatial considerations of pedestrians. On the contrary, SSEs are only associated with certain environments or certain social rules of human society. Both kinds of spatial effects often co-exist and affect pedestrian behaviors at the same time.

We propose a framework, called SBCM, to describe the relationships between pedestrian behaviors and environments. It consists of two main parts, the pedestrian model and SSE database. The architecture of SBCM is shown in Fig. 5. The pedestrian model retains all the spatial effects associated with current environment. Thus GSEs always exist in pedestrian model and SSEs are only considered while associated features are detected in the environments. The pedestrian behaviors are represented by fusing the spatial effects in the pedestrian model.

However, there are two difficulties for building SBCM. The first is correctly integrating different spatial effects. To solve this problem, we model pedestrian behaviors as Markov decision processes and estimate the cost weighting of each spatial effect by inverse reinforcement learning (IRL) [11].

The second difficulty is to detect and learn the new SSEs in the environments. Our proposed idea is to learn a general behavior model which only engages with GSEs at first. Then this general behavior model helps to detect the SSE. The SSE can be further identified and learned by "subtracting" GSEs from pedestrian behaviors. The learned SSE is stored in SSE database and can be used to model pedestrian behaviors or detect new SSEs while the associated feature of learned SSE appears in the environments. The section IV and V will further discuss the cost functions of GSEs and SSEs. The IRL for cost learning is also introduced in each section.

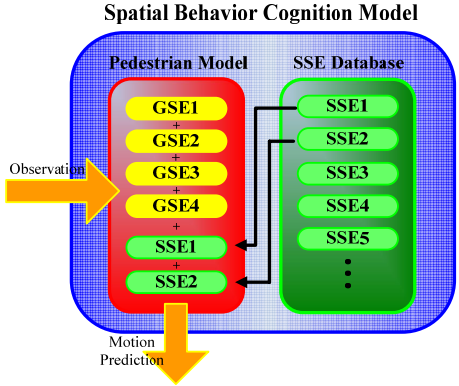

Fig. 5 Spatial behavior cognition model

IV. GENERAL SPATIAL EFFECT LEARNING

We assume that pedestrian spatial behaviors influenced by four GSEs (trajectory length, static obstacle, moving obstacle, constant steering). Each GSE associates with a cost function C_i for pedestrian state o_k in time step k. The cost function under GSEs, C_{GSE}, is written as a linear combination of C_i with different weights w_i shown as Eq(1). The following sections describe the formulation of each cost function.

$$C_{GSE}(o_k) = w_{des}C_{des}(o_k) + w_{obs}C_{obs}(o_k) + w_{mo}C_{mo}(o_k) + w_{str}C_{str}(o_k) \quad (1)$$

A. Trajectory Length

We hypothesize that all pedestrians have certain destinations and move toward destinations with "pedestrian policy." The trajectory length which indicates the distance from the current location of the pedestrian to the destination is regarded as a type of cost. Thus the cost function to the destination C_{des} can be described by Euclidean distance ($dist(\cdot)$) between two sequential states.

$$C_{des}(o_k) = dist(o_k - o_{k-1}) \quad (2)$$

B. Static Obstacles

In general, pedestrians would like to avoid obstacles for safety. Thus obstacles can be viewed as a repulsive force that generates high cost while pedestrians are closed to it. Distance transform (Dist) is used to obtain the closest distance to obstacles (Fig. 6(a)). Moreover, we adopt the similar formulation in [13] for the cost function C_{obs}. σ is defined as 0.361 estimated from [13].

$$C_{obs}(o_k) = \exp(-0.5 \cdot Dist(o_k)^2 / \sigma^2) \quad (3)$$

C. Moving Obstacles

Hall [5] demonstrated that personal space (PS) plays an important role in spatial interactions between humans. PS can be considered as a self-own area surrounding each person. The violation of PS often causes emotional reactions depending on the relation between two persons. PS usually forms as an elliptic shape shown in Fig. 6(b). In this paper, the concept of PS also helps to formulate the cost caused from other pedestrians. According to [1], PS around the pedestrian can be modeled as a combination of 2 two-dimensional Gaussian functions shown in Fig. 6(b). The cost function of pedestrian i suffered from other pedestrians, C_{mo}, can be described as the summation of cost from pedestrian j to pedestrian i, C_{ji}, shown in Eq.(4).

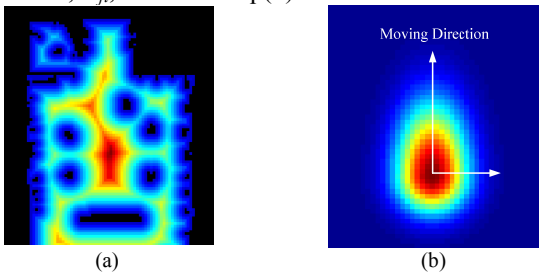

(a) (b)

Fig. 6 (a) Distance transform (Dist). The obstacle is displayed as black color. The original map is shown in Fig. 7, (b) the cost function of personal space.

$$C_{mo}(o_k^i) = \sum_j C_{ji} = \sum_j \exp\left(-0.5 \cdot (o_k^j - o_k^i)^t \Sigma^{-1} (o_k^j - o_k^i)\right) \quad (4)$$

if j is in front of i $\Sigma = \begin{pmatrix} \sigma^2 & 0 \\ 0 & 4\sigma^2 \end{pmatrix}$, others $\Sigma = \begin{pmatrix} \sigma^2 & 0 \\ 0 & \sigma^2 \end{pmatrix}$. σ is also defined as 0.361 in this paper.

D. Constant Steering

Since pedestrians usually avoid frequently changing moving directions, the last cost function of GSE is to penalize the steering variation as shown in Eq.(5).

$$C_{str}(o_k) = \left(steering(o_k) - steering(o_{k-1})\right)^2 \quad (5)$$

E. Model Learning

We assume the pedestrian spatial behaviors can be represented as a MDP. The pedestrian trajectory consisting of sequential discrete states (o_0, o_1, o_2…) follows the pedestrian policy π_p. The value function V for the policy π evaluated at pedestrian state o_0 is given by Eq.(6).

$$V^{\pi}(o_0) = C(o_0) + \gamma C(o_1) + \gamma^2 C(o_2) + \cdots \quad (6)$$

Where $\gamma \in [0,1)$ is the discount factor. $C(o_k)$ is the total cost at state o_k.

In this section, since the pedestrian model only considers GSEs, $C(o_k)$ is equal to $C_{GSE}(o_k)$. Our purpose is to estimate the parameter w_i under the pedestrian policy. This estimation can be viewed as an inverse reinforcement learning (IRL) problem. We adopt the method [11] which formulates IRL as maximizing the difference of quality between the observed policy and other policies. The optimization can be efficiently solved by linear programming methods. Here the optimization problem becomes

$$\max \sum_{o_0 \in X_0} \sum_j \left(V^{\pi_j}(o_0) - V^{\pi_p}(o_0)\right) - \lambda \cdot w_i \quad (7)$$

$$s.t. \quad \lambda \geq 1, \quad 0 < w_i \leq w_{\max}, \quad V^{\pi_j}(o_0) \geq V^{\pi_p}(o_0)$$

X_0 is the set of initial states of pedestrian trajectories. λ is the penalty to prevent large w_i. Several policies π_j, which separately consider C_{des}, C_{obs}, or randomly combination of other cost functions, generate different trajectories for $V^{\pi_j}(o_0)$. The model evaluation for GSEs is discussed in section VII.

V. SPECIFIC SPATIAL EFFECT LEARNING

However, some spatial effects only appear in certain environments or from certain objects and cannot be described by GSEs. SSEs help to compensate this part. SSEs are regarded as the additional spatial effects to influence pedestrian behaviors. If the cost function C represents the cost of observed pedestrian behaviors, we are able to detect SSEs and even further estimate SSEs by subtracting GSEs from the cost function C. The complete cost function C can be written as

$$C(o_k) = C_{GSE}(o_k) + C_{SSE}(o_k) \quad (8)$$

$C_{GSE}(o_k)$ is available from Eq.(1). The cost function C_{SSE} is

represented as a grid map tabulating the costs of the SSE in discrete locations (Fig. 8 (a)). Similar to the last section, the cost estimation can be transformed into an optimization problem shown in Eq.(9). *Hist(s)*, which records the frequency of pedestrian passing location *s*, is also provided as the penalty term. One thing we should notice is that only the parameters of the SSE are estimated in Eq.(9), the parameters of GSEs are reserved. Moreover, we generate several C_{SSE} by slightly translating the coordinate of C_{SSE} to different locations (Fig. 8 (b)). After fusing these C_{SSE}, a high resolution C_{SSE} is available.

$$\max \sum_{o_0 \in X_0} \sum_{j} \left(V^{\pi_j}(o_0) - V^{\pi_p}(o_0) \right) - \lambda \cdot Hist(s) \cdot C_{SSE}(s) \quad (9)$$

$$s.t. \quad \lambda > 0, \quad 0 \le C_{SSE}(s) \le C_{\max}, \quad V^{\pi_j}(o_0) \ge V^{\pi_p}(o_0)$$

Where *s* indicates all the discrete states in the grid map.

A simple experiment is designed to verify the idea. Five destinations and the grid map of the environment are shown in Fig. 7. An interactive exhibition locates in the center of the environments. The pedestrians are not allowed to go into the interactive area in this case. However, the robot equipped with a laser range finder cannot detect the interactive area from the grid map and also cannot model the forbidden behavior from GSEs. It is required to detect and learn this SSE (the forbidden behavior) from the observed pedestrian trajectories.

44 pedestrian trajectories are collected while 30 trajectories are detected as unusual by the pedestrian model only considering GSEs (Fig. 9(a)). Fig. 9(b) demonstrates the histogram *Hist(s)* of pedestrian trajectories. The cost function of SSE, C_{SSE}, is further estimated by Eq.(9). The estimated results are displayed in Fig. 10. The result of estimated C_{SSE} without *Hist(s)* is also shown for comparison. After adding C_{SSE} to the pedestrian model, SBCM generates the new pedestrian policy. The policy of the before and the after considering SSE are illustrated in Fig. 11. The policy considering the SSE is closer to the pedestrian policy.

VI. Probability Framework

In this section, the probability model of prediction is derived. To clarify the meaning of symbols, some symbols are defined as follows. O_k is represented as the pedestrian trajectory from time step 1 to *k*.

$$O_k \triangleq \{o_1, o_2, \cdots o_k\} \quad (10)$$

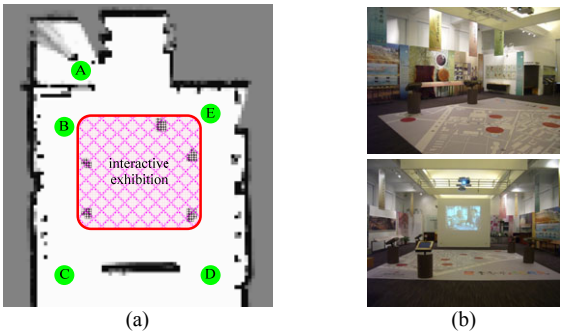

(a) (b)

Fig. 7 History gallery, (a) the interactive exhibition is in the center of the map and 5 destinations are denoted as green circles, (b) environment pictures.

o_k^g indicates the discrete states of the pedestrian at time step *k*. *G* describes the destination of the pedestrian. The prediction of behaviors consists of short term and long term prediction. In short term prediction, only the area within PEG is concerned while the long term prediction considers the areas out of the PEG. In the following paragraphs, three situations, short term prediction, long term prediction and multiple destinations are discussed.

A. Short term prediction

The probability model of short term prediction is represented as $p(o_{k+T} | o_k, G)$. Here we assume the pedestrian takes *T* time steps to walk through the PEG area. The probability is obtained from the statistical results that compare the predicted trajectory with real pedestrian trajectories.

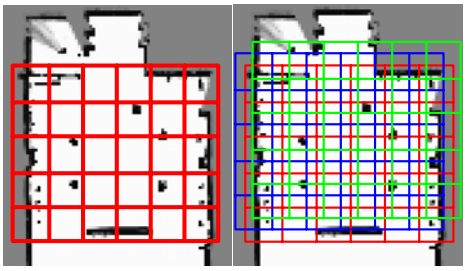

(a) (b)

Fig. 8 (a) The cost function is represented as the discrete states, (b) fusing multiple learned cost functions to generate one high resolution cost function

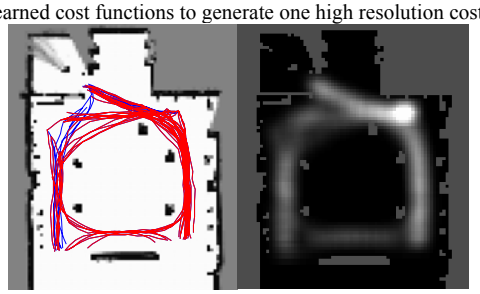

(a) (b)

Fig. 9 (a) unusual trajectories are shown in red color, (b) *Hist(s)*.

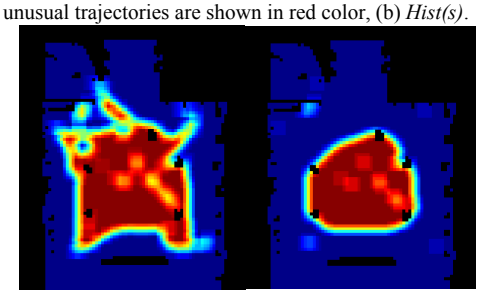

(a) (b)

Fig. 10 Cost function of SSE, (a)without *Hist(s)*, (b) with *Hist(s)*.

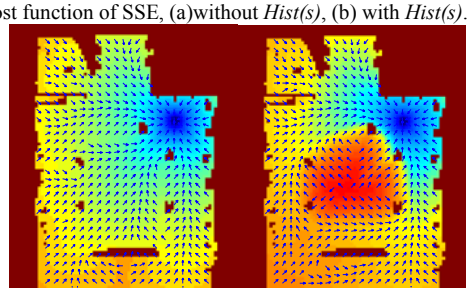

(a) (b)

Fig. 11 Pedestrian policies for destination E, (a) without SSE, (b) with SSE.

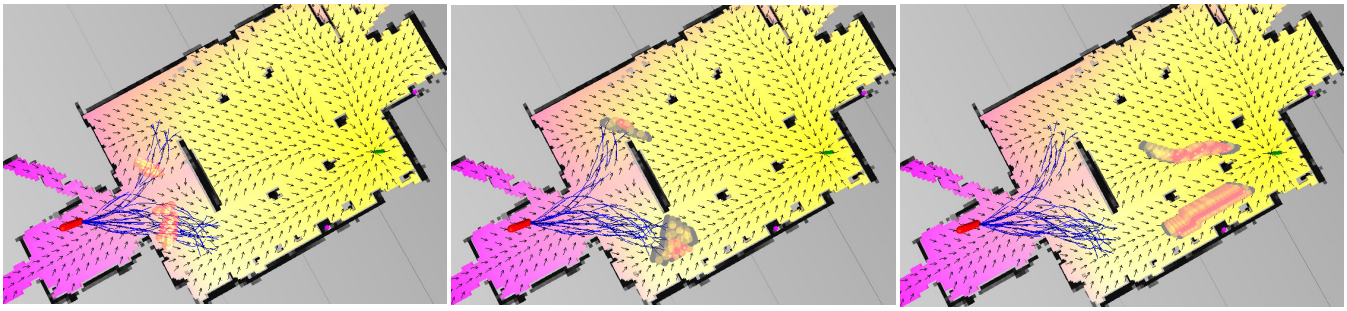

(a) (b) (c)

Fig. 12 Simulation of long term prediction in different time steps, (a) t = 3 s, (b) t = 5 s, (c) t = 9 s.

B. Long term prediction

In the long term prediction, the prediction result is represented in discrete state in grid map. The probability of the prediction from time step k to $k+N$ is modeled as $p\left(o^g_{k+N} \mid o_k, G\right)$. According to the total probability, it is factorized as

$$\begin{aligned} p\left(o^g_{k+N} \mid o_k, G\right) &= \sum_{o^g_{k+N-1}} p\left(o^g_{k+N} \mid o^g_{k+N-1}, G\right) p\left(o^g_{k+N-1} \mid o_k, G\right) \\ &= \prod_{i=k+T+1}^{k+N-1} \left(\sum_{o^g_i} p\left(o^g_{i+1} \mid o^g_i, G\right) \right) \cdot \sum_{o^g_{k+T}} p\left(o^g_{k+T+1} \mid o^g_{k+T}, G\right) p\left(o^g_{k+T} \mid o_k, G\right) \end{aligned} \tag{11}$$

Each grid state has 16 directions toward its next states. Thus we can utilize similar estimation method as short term prediction to estimate $p\left(o^g_{i+1} \mid o^g_i, G\right)$. The final term $p\left(o^g_{k+T} \mid o_k, G\right)$ of Eq.(11) can be derived to the summation of the multiplication of state discretization and the short term prediction as shown in Eq. (12). Fig. 12 shows the simulation result.

$$p\left(o^g_{k+T} \mid o_k, G\right) = \sum_{o_{k+T}} \underbrace{p\left(o^g_{k+T} \mid o_{k+T}\right)}_{\text{discretization}} \underbrace{p\left(o_{k+T} \mid o_k, G\right)}_{\text{short term prediction}} \tag{12}$$

C. Multiple destinations

In general, the destination of the pedestrian is usually unknown. However, we are able to derive the weightings of different destinations from the pedestrian trajectory. By Bayes rule, the posterior of goal weighting $p(G_k|O_k)$ in time step k can be described as the multiplication of one step prediction and goal weighting in time step k-1. In other words, it is able to iteratively estimate the goal weighting while the new information of the pedestrian is available.

$$\begin{aligned} p\left(G_k \mid O_k\right) &\propto p\left(o_k \mid o_{k-1}, G_k\right) p\left(G_k \mid O_{k-1}\right) \\ &= p\left(o_k \mid o_{k-1}, G_k\right) p\left(G_{k-1} \mid O_{k-1}\right) \end{aligned} \tag{13}$$

Based on the pedestrian trajectory O_k, a generalized long term prediction model $p\left(o^g_{k+N} \mid O_k\right)$ in multiple destinations environments is represented by the combination of individual long term pedestrian models with different weights shown as

$$\begin{aligned} p\left(o^g_{k+N} \mid O_k\right) &= \sum_i^m p\left(o^g_{k+N} \mid O_k, G^i_k\right) p\left(G^i_k \mid O_k\right) \\ &= \sum_i^m \underbrace{p\left(o^g_{k+N} \mid o_k, G^i_k\right)}_{\text{Prediction}} \underbrace{p\left(G^i_k \mid O_k\right)}_{\text{Goal Weighting}} \end{aligned} \tag{14}$$

VII. Model Evaluation and Robot Experiment

A. Model Evaluation

In the training phase, 233 trajectories are collected from one outdoor (seq_eth) [15] and two indoor environments.

In the testing phase, the trajectories of PEG are scored and prioritized on-line by V^π as shown in Eq.(6). The trajectory with the lowest value of V^π is chosen as the predicted trajectory of the pedestrian. However, the scores of the first several prioritized trajectories usually have a slight difference. In other words, they all have large chances of being chosen by pedestrians. To demonstrate the characteristic of multiple hypotheses, PEG is represented in three different types: PEG1, PEG5, and PEG10. The number indicates the amount of prioritized trajectories in PEG compared to the ground truth. The best one is chosen as the evaluated trajectory. For example, PEG5 means that the evaluated trajectory is the best matching trajectory chosen from the first five prioritized trajectories.

Moreover, PEG is also evaluated by comparing with other pedestrian models including constant velocity (CV) and linear trajectory avoidance (LTA) [13]. 80 testing trajectories are randomly selected from the dataset (seq_hotel) [15]. However, the trajectories of short length or those belonging to a group are removed. The prediction results are shown in Fig. 13. The average error and its one standard deviation in different distances of prediction are listed in TABLE I and TABLE II. All the models perform well while predicted distance is lower than 3 meters. However, performance difference is obvious in long distance prediction. Because of the advantage of multiple hypotheses, PEG5 and PEG10 dramatically decrease the prediction error and shrink the uncertainty of prediction.

B. Robot Experiment

This section demonstrates a service robot performs pedestrian-like motions by considering the spatial effects discussed in section IV and V. The robot platform is shown in Fig. 14(a). The laser ranger finder equipped on the robot is used for localization and pedestrian tracking. By learning the spatial effects, the robot is able to search a path similar to the pedestrian behavior that detours around the interactive exhibition (Fig. 14(b)). While a pedestrian is moving toward the right-bottom side of the map, the robot is able to utilize

the pedestrian model to predict the potential location of the pedestrian in the next few seconds. To prevent the potential collision, the robot queries a new path surrounding the other side of the interactive exhibition (Fig. 14 (c)-(d)).

VIII. Conclusion

In this paper, we present the concept of pedestrian ego-graph (PEG) and the framework of spatial behavior cognition model (SBCM). PEG provides human-like trajectories for modeling pedestrian behaviors. By the advantages of multiple hypotheses, PEG is helpful to build the probability model of prediction. Moreover, the proposed framework of SBCM not only provides a good ability to discover new spatial effects but also estimates the corresponding cost functions. Furthermore, the probability models of prediction including short term, long term and multiple destinations are also derived. The pedestrian model combining PEG and SBCM shows excellent results in the model evaluation. Finally, we have further demonstrated a practical application that a service robot behaves socially acceptable motions by detecting and learning the spatial effects in the environment.

References

[1] T. Amaoka, H. Laga, S. Saito, and M. Nakajima, "Personal Space Modeling for Human-Computer Interaction," *Proc. 8th Int. Conf. on Entertainment Computing*, Paris, France, pp. 60-72, 2009.

[2] M. Bennewitz, W. Burgard, G. Cielniak, and S. Thrun, "Learning Motion Patterns of People for Compliant Robot Motion," *Int. J. Robotics Research,* vol. 24, pp. 31-48, 2005.

[3] D. Ellis, E. Sommerlade, and I. Reid, "Modelling Pedestrian Trajectories with Gaussian Processes," *9th Int. Workshop on Visual Surveillance*, Kyoto, Japan, 2009.

[4] S. Gaffney and P. Smyth, "Trajectory Clustering with Mixtures of Regression Models," *Proc. of the 5th ACM SIGKDD int. conf. on Knowledge discovery and data mining*, San Diego, CA, USA, pp. 63-72, 1999.

[5] E. T. Hall, *The Hidden Dimension*. Anchor Books, 1966.

[6] D. Helbing and P. Molnár, "Social Force Model for Pedestrian Dynamics," *Physical Review E,* vol. 51, pp. 4282-4286, 1995.

[7] T. M. Howard and A. Kelly, "Optimal Rough Terrain Trajectory Generation for Wheeled Mobile Robots," *Int. J. Robotics Research,* vol. 26, pp. 141-166, 2007.

[8] T. Kanda, D. F. Glas, M. F. Shiomi, and N. F. Hagita, "Abstracting People's Trajectories for Social Robots to Proactively Approach Customers," *IEEE Trans. on Robotics,* vol. 25, pp. 1382-1396, 2009.

[9] A. Lacaze, Y. Moscovitz, N. DeClaris, and K. Murphy, "Path Planning for Autonomous Vehicles Driving over Rough Terrain," *Proc. IEEE Int. Sym. on Intelligent Control*, Gaithersburg, MD, USA, pp. 50-55, 1998.

[10] Y. Nakauchi and R. Simmons, "A Social Robot That Stands in Line," *Autonomous Robots,* vol. 12, pp. 313-324, 2002.

[11] A. Y. Ng and S. J. Russell, "Algorithms for Inverse Reinforcement Learning," *Proc. of the Seventeenth Int. Conf. on Machine Learning*, Stanford, CA, USA, pp. 663-670, 2000.

[12] E. Pacchierotti, H. I. Christensen, and P. Jensfelt, "Evaluation of Passing Distance for Social Robots," *Proc. The 15th IEEE Int. Sym. on Robot and Human Interactive Communication*, Hatfield, UK, pp. 315-320, 2006.

[13] S. Pellegrini, A. Ess, K. Schindler, and L. v. Gool, "You'll Never Walk Alone: Modeling Social Behavior for Multi-Target Tracking," *Proc. IEEE Int. Conf. on Computer Vision*, Kyoto, Japan, pp. 261-268, 2009.

[14] B. Ziebart, N. Ratliff, G. Gallagher, C. Mertz, K. Peterson, J. A. Bagnell, M. Hebert, A. Dey, and S. Srinivasa, "Planning-Based Prediction for Pedestrians," *Proc. IEEE Int. Conf. on Intelligent Robots and Systems*, St. Louis, MO, USA, pp. 3931-3936, 2009.

[15] http://www.vision.ee.ethz.ch/datasets/

TABLE I
STATISTICAL RESULTS- AVERAGE ERROR (UNIT:METER)

	1 m	2 m	3 m	4 m	5 m	6 m	7 m
CV	0.0373	0.1221	0.2210	0.3625	0.5272	0.6890	0.8540
LTA	0.0535	0.1279	0.2119	0.2850	0.3779	0.4443	0.5087
PEG1	0.0475	0.1347	0.2226	0.3034	0.3417	0.3801	0.4432
PEG5	0.0306	0.0754	0.1058	0.1174	0.1310	0.1561	0.2326
PEG10	0.0294	0.0744	0.1000	0.1045	0.1209	0.1338	0.2050

TABLE II
STATISTICAL RESULTS- STANDARD DEVIATION (UNIT:METER)

	1 m	2 m	3 m	4 m	5 m	6 m	7 m
CV	0.0420	0.1554	0.2590	0.3883	0.5274	0.6867	0.8984
LTA	0.0431	0.0921	0.1499	0.2036	0.2475	0.3067	0.3754
PEG1	0.0469	0.1352	0.1544	0.2168	0.2629	0.3188	0.3649
PEG5	0.0290	0.0559	0.0764	0.1026	0.1400	0.1674	0.1989
PEG10	0.0259	0.0567	0.0665	0.0828	0.1264	0.1605	0.1740

Fig. 13 Prediction results in different pedestrian models. The right image shows LTA fails in the area with local minimum cost. Black: ground truth. Red: PEG. Blue: LTA. Green: CV

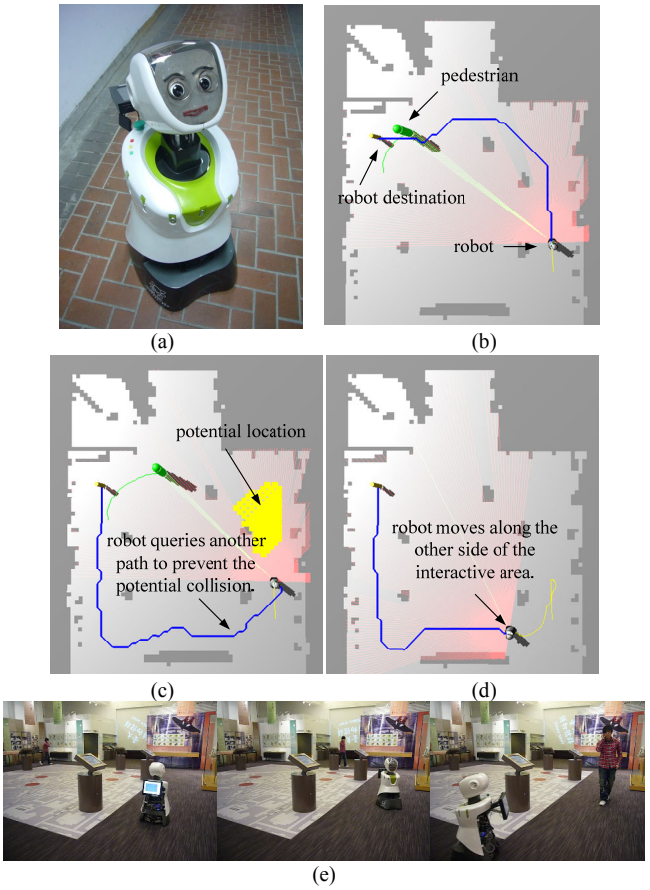

Fig. 14 the experiment of navigation.